SUPPORTING INFORMATION

One-electron-reduction of 8-bromoisoguanosine and 8-bromoxanthosine in the aqueous phase: Step-by-step vs concerted proton-coupled electron routes

Chryssostomos Chatgilialoglu, Mila D'Angelantonio, Panagiotis Kaloudis, Quinto G. Mulazzani and Maurizio Guerra**

ISOF, Consiglio Nazionale delle Ricerche, Via P. Gobetti 101, 40129 Bologna, Italy.

Materials

Isoguanosine. To a solution of 2,6-diaminopurine (282 mg, 1.00 mmol) and $NaNO_2$ (311 mg, 4.5 mmol) in water (7 mL) at 50°C, acetic acid (400 µL, 7.00 mmol) was added dropwise under stirring during 2 min. The mixture was further stirred for 5 min and diluted with water (10 mL). Conc. 25% aq. NH_3 (8 mL) was added, the mixture was stirred for 10 min and evaporated to dryness. The residue was applied onto a column packed with Dowex 50W x 8, washed with water (200 mL) and the product was eluted with 10% aq. NH_3 (200 mL) as brownish flakes (185 mg, 65%). ^{1}H-NMR (400 MHz, DMSO-d6) δ 3.51 (dd, 1H, $J_{5'',}$ = 12.3, $J_{4'}$ = 2.6 Hz, H-5') 3.61 (dd, 1H, $J_{5'}$ = 12.3, $J_{4'}$ = 2.6 Hz, H-5'') 3.93 (dd, 1H, $J_{3'}$ = 4.4, $J_{5'}$ = 2.6 Hz, H-4') 4.06 (dd, 1H, $J_{4'}$ = 4.4, $J_{2'}$ = 2.5 Hz, H-3') 4.47 (dd, 1H, $J_{1'}$ = 6.5, $J_{3'}$ = 2.5 Hz, H-2') 5.62 (d, 1H, $J_{2'}$ = 6.5 Hz, H-1') 7.94 ppm (s, 1H, H-8). ^{13}C-NMR (100 MHz, DMSO-d6) δ 61.7 (C-5') 70.8 (C-2') 72.8 (C-3') 86.0 (C-4') 87.6 (C-1') 109.5 (C-5) 131.5 (C-4) 138.3 (C-8) 152.0 (C-2) 155.6 ppm (C-6). MS (+ESI): *m/z* 283.9 $[M+H]^+$.

8-Bromoisoguanosine. To a suspension of isoguanosine (50 mg, 0.18 mmol) in water (0.5 mL) were added 1.5 mL of a saturated aqueous Br_2 solution dropwise during 15 min. The reaction mixture was stirred for 1 h at room temperature and a 5 M sodium bisulfite solution was added until the color of the reaction mixture changes from red to yellow. The pH of the solution was adjusted to 6-7 with 1 M NaOH, the solution was evaporated to half of its volume and it was left overnight in the refrigerator. The precipitated crystals were filtered, washed with water (1 mL) and acetone (1 mL) and recrystallized from water to afford 33 mg of 8-bromoisoguanosine as a yellowish solid (51%). ^{1}H-NMR (400 MHz, DMSO-d6) δ 3.47 (dd, 1H, $J_{5'',}$ = 11.4, $J_{4'}$ = 2.8 Hz, H-5') 3.63 (dd, 1H, $J_{5'}$ = 11.4, $J_{4'}$ = 2.8 Hz, H-5'') 3.94 (dd, 1H, H-4') 4.09 (dd, 1H, H-3') 4.99 (dd, 1H, H-2') 5.64 (d, 1H, $J_{2'}$ = 6.9 Hz, H-1') 5.96 (bs, 2H, NH_2) 10.83 ppm (bs, 1H, NH). ^{13}C-NMR (100 MHz, DMSO-d6) δ 62.3 (C-5') 70.6

(C-2') 71.1 (C-3') 87.1 (C-4') 90.1 (C-1') 109.7 (C-5) 123.6 (C-8) 150.9 (C-4) 154.9 (C-2) 155.4 ppm (C-6). MS (+ESI): *m/z* 361.8 $[M+H]^+$.

8-Bromoxanthosine. To a suspension of xanthosine (500 mg, 1.76 mmol) in water (5 mL) were added 15 mL of a saturated aqueous Br_2 solution dropwise during 20 min. The reaction mixture was stirred for 1 h at 40°C, cooled and the precipitated crystals were filtered, washed with water (2 mL) and recrystallized from water to afford 430 mg of 8-bromoxanthosine as a white powder (67%). ^{1}H-NMR (400 MHz, DMSO-d6) δ 3.70 (dd, 1H, $J_{5''}$ = 12.1, $J_{4'}$ = 2.2 Hz, H-5') 3.75 (dd, 1H, $J_{5'}$ = 12.1 $J_{4'}$ = 2.2 Hz, H-5'') 4.06 (dd, 1H, H-4') 4.09 (dd, 1H, H-3') 4.25 (dd, 1H, $J_{1'}$ = 6.2, $J_{3'}$ = 2.8 Hz, H-2') 5.40 (d, 1H, OH) 5.64 (d, 1H, $J_{2'}$ = 6.2 Hz, H-1') 5.74 (d, 1H, OH) 6.93 (bs, 1H, NH) 11.03 ppm (bs, 1H, NH). ^{13}C-NMR (100 MHz, DMSO-d6) δ 61.0 (C-5') 70.9 (C-2') 72.9 (C-3') 86.3 (C-1') 90.8 (C-4') 116.4 (C-5) 119.4 (C-8) 140.0 (C-4) 150.0 (C-2) 156.8 ppm (C-6). MS (+ESI): *m/z* 384.7 $[M+Na]^+$.

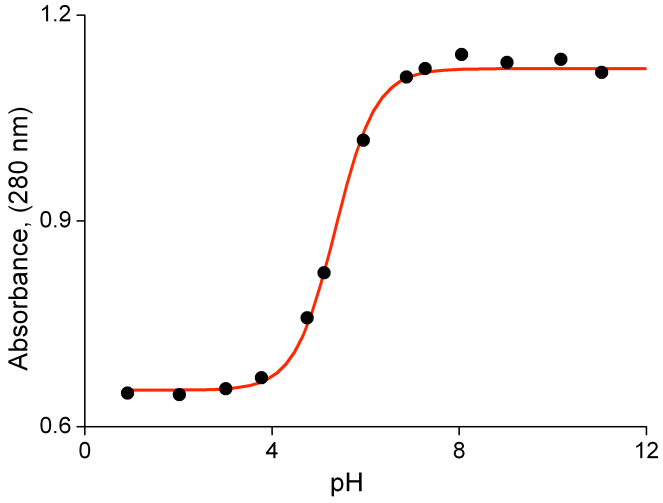

Figure S1. pH dependence of absorption at 280 nm obtained from solutions containing 1.0 mM 8-bromoxanthosine. The solid line represents the pK_a equation fit to the data; the inflection point was obtained at pH = 5.4.

Pulse Radiolysis

Pulse radiolysis with optical absorption detection was performed by using a 12 MeV linear accelerator, which delivered 20 -200 ns electron pulses with doses between 5 and 50 Gy, by which $OH^{\bullet}$, $H^{\bullet}$ and e_{aq}^{-} are generated with 1-20 μM concentrations.[1] The pulse irradiations were performed at room temperature (22 ± 2 °C) on samples contained in Spectrosil quartz cells of 2 cm optical path length. Solutions were protected from the analyzing light by means of a shutter and appropriate cutoff filters. The bandwidth used throughout the pulse radiolysis experiments was 5 nm. The radiation dose per pulse was monitored by means of a charge collector placed behind the irradiation cell and calibrated with an N_2O-saturated solution containing 0.1 M HCO_2^- and 0.5 mM methylviologen, using $G\varepsilon = 9.66 \times 10^{-4}$ m^2 J^{-1} at 602 nm.[2] G(X) represents the number of moles of species X formed, consumed or altered per joule of energy absorbed by the system.

Radiolysis of neutral water leads to e_{aq}^{-}, $HO^{\bullet}$ and $H^{\bullet}$ as shown in eq 1. The values in parentheses represent the radiation chemical yields (G) in units of μmol J^{-1}. The reactions of e_{aq}^{-} with the substrates were studied in O_2–free solutions containing 0.25 M *t*-BuOH. Based on the available kinetic data, we expected that $HO^{\bullet}$ is scavenged efficiently (eq 2, $k_2 = 6.0 \times 10^8$ M^{-1} s^{-1}), whereas $H^{\bullet}$ is trapped only partially (eq 3, $k_3 = 1.7 \times 10^5$ M^{-1} s^{-1}) under the utilized concentrations of *t*-BuOH.[3,4]

$$H_2O \xrightarrow{\sim\sim} e_{aq}^{-}(0.27), HO^{\bullet}(0.28), H^{\bullet}(0.062) \qquad (1)$$

$$HO^{\bullet} + t\text{-BuOH} \rightarrow (CH_3)_2C(OH)CH_2^{\bullet} + H_2O \qquad (2)$$

$$H^{\bullet} + t\text{-BuOH} \rightarrow (CH_3)_2C(OH)CH_2^{\bullet} + H_2 \qquad (3)$$

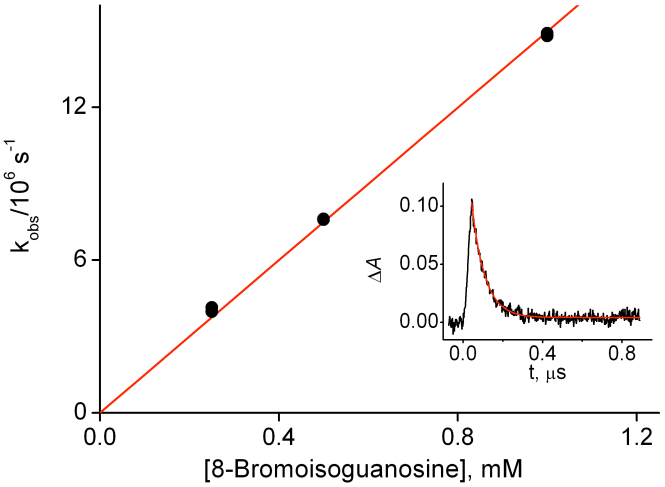

Figure S2. Plot of k_{obs} vs [8-bromoisoguanosine] for the decay of e_{aq}^- (λ = 720 nm) from the pulse radiolysis of Ar-purged solutions containing 0.25 M *t*-BuOH at pH 7. Inset: Decay observed at 720 nm in the presence of 1.0 mM 8-bromoisoguanosine; optical path = 2.0 cm, dose per pulse 12.4 Gy. The solid line represents the first-order kinetic fit to the data

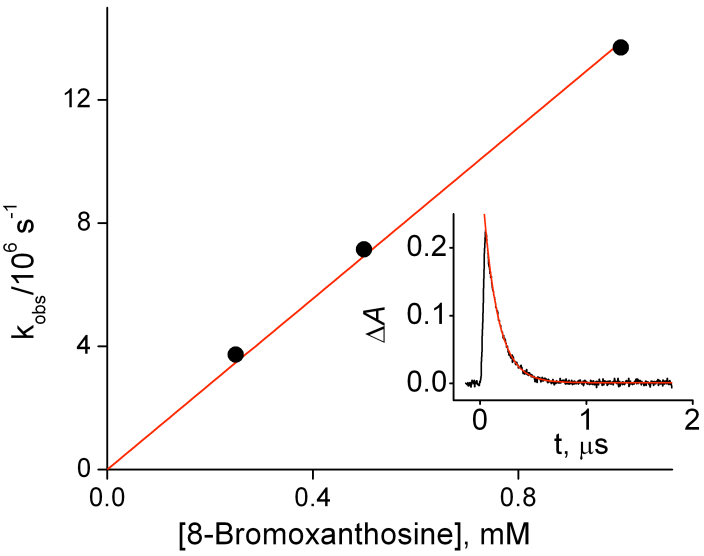

Figure S3. Plot of k_{obs} vs [8-bromoxanthosine] for the decay of e_{aq}^- (λ = 720 nm) from the pulse radiolysis of Ar-purged solutions containing 0.25 M *t*-BuOH at pH 4.2. Inset: Decay observed at 720 nm in the presence of 0.5 mM 8-bromoxanthosine; optical path = 2.0 cm, dose per pulse 24.4 Gy. The solid line represents the first-order kinetic fit to the data.

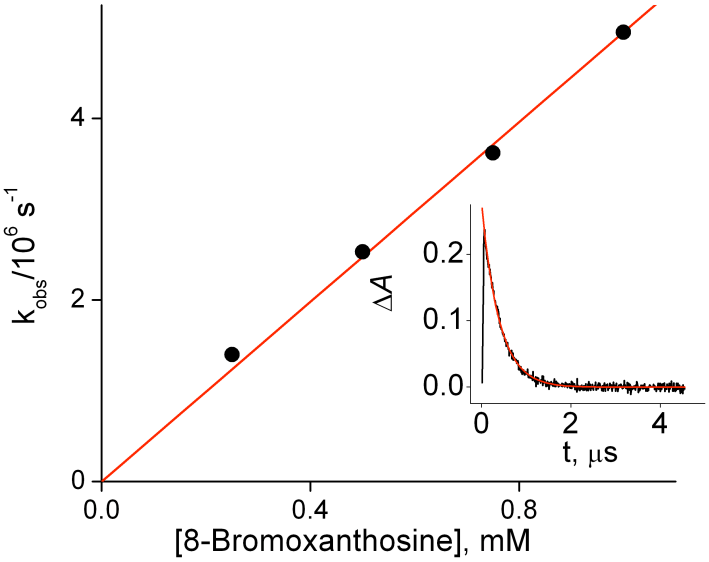

Figure S4. Plot of k_{obs} vs [8-bromoxanthosine] for the decay of e_{aq}^- (λ = 720 nm) from the pulse radiolysis of Ar-purged solutions containing 0.25 M *t*-BuOH at pH 7.6. Inset: Decay observed at 720 nm in the presence of 0.5 mM 8-bromoxanthosine; optical path = 2.0 cm, dose per pulse 24.4 Gy. The solid line represents the first-order kinetic fit to the data.

DFT Calculations

DFT calculations at the B1B95/6-31+(λ=0.7)G** level were performed on 9-methyl-8-bromoisoguanine (**1**), 9-methyl-8-bromoxanthine (**2**) and its deprotonated form **3** to determine the stability of their radical anions and to assign the tautomeric form of the observed intermediates.

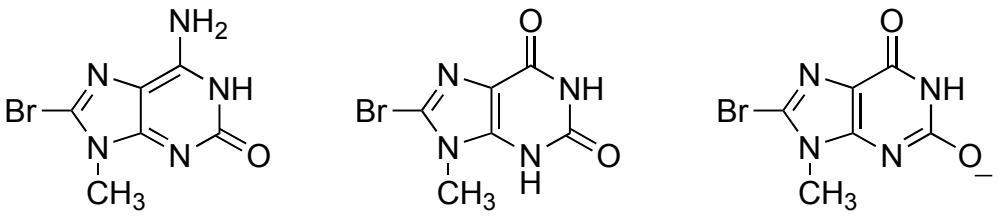

1 **2** **3**

Calculations show that the radical anion of **1** is stable as found previously for the corresponding derivative of guanine so that 8-bromoisoguanosine should afford the deprotonated radical cation of isoguanosine in accord with experiment. Tautomers **4** and **5** can be obtained by deprotonation, respectively at N1 (aminic form) and at the amino group (iminic form). To identify the species responsible of the absorption spectrum observed during pulse radiolysis (see Figure 1), the experimental absorption bands are compared with those computed with the time-dependent DFT method (TD-B3LYP/6-311G**) since this theoretical method was previously found by us to provide reliable optical transitions in nucleosides.[5-7]

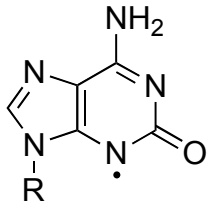

4

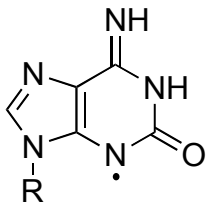

5

Calculations reported in Table S1 suggest that deprotonation occurs at N1. Indeed, the computed spectrum for the aminic tautomer **4** is in rather good accord with the experimental one (λ_{max} at *ca*. 300 nm, a shoulder at 360 nm, weak bands at 500 and 600nm). On the other hand, agreement with experiment worsens for the iminic tautomer **5** since a weak optical transition about 500 nm is lacking in the computed spectrum.

Table S1 TD-B3LYP/6-311G**//B1B95/6-31+G** optical transitions for the various tautomeric forms of deprotonated one-electron oxidized 9-methylisoguanine.

Radical	λ/nm	f
4	294	0.115
	348	0.031
	430	0.030
	695	0.014
5	288	0.079
	338	0.043
	678	0.023

DFT calculations carried out on radical anion of **2** indicate that in this case the radical anion is not stable and tend to lose Br^- as previously found for the 8-bromoadenine derivatives so that electron capture in 8-bromoxanthosine should lead to C5'-C8 cyclization. The scenario changes dramatically with the monoanion **3**. Indeed, electron capture produces a dianion that should instantaneously be protonated. Interestingly, optimization of the dianion that interacts with a hydrogen atom located 2.0 Å above the C8 atom (see Figure 4A) leads to radical **6** that interacts with Br^- (see Figure 4B), the C8-Br distance being 2.84 Å and the Mulliken atomic charge at Br being computed to be –0.65e.

6

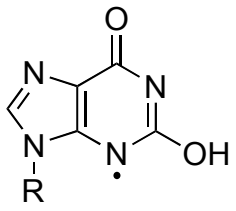

7

The optical spectra of tautomers **6** and **7** were computed at the TD-B3LYP/6-311G**//B1B95/6-31+G** level in order to further confirm the observed intermediate. Table S2 shows

that the computed spectra are similar and in rather good accord with the experimental spectrum (λ_{max} at 300 nm, a shoulder at 370 nm and a weak broad band at 480 nm), however in **7** is present a transition at 693 nm that is absent in the experimental spectrum. This finding suggests that the absorption spectrum observed during pulse radiolysis should be assigned to the ribo derivative of **6**.

Table S2. TD-B3LYP/6-311G**//B1B95/6-31+G** optical transitions for the various tautomeric forms of deprotonated one-electron oxidized 9-methylxanthine.

Radical	λ/nm	*f*
6	281	0.087
	348	0.057
	455	0.014
	528	0.017
7	283	0.052
	322	0.039
	476	0.015
	693	0.015

Computational details. Hybrid meta DFT calculations with the B1B95 (Becke88[8]-Becke95[9] 1-parameter model for thermochemistry) functional[10] were carried out using the Gaussian 03 system of programs[11] This HMDFT model was found to give excellent performance for thermochemistry[12], molecular geometries[12,13] as well as for electron affinities.[13] Unrestricted wavefunction was used for radical species. Optimized geometries and total energies were obtained employing the valence double-ζ basis set supplemented with polarization functions and augmented with moderate (λ=0.7) diffuse functions on heavy atoms that were found[14,15] to provide reliable results on radical anions that are unstable in the gas phase. Indeed the criterions outlined in ref. 15 are fully satisfied. Hence the B1B95 calculations on Br derivatives were carried out using the 6-31+(λ=0.7)G** basis set. Relative energies

were corrected for the zero point vibrational energy (ZPVE) computed from frequency calculations using a scaling factor of 0.9735 to account for anharmonicity.[12] The nature of the ground states (zero imaginary frequency) was verified by frequency calculations. The B3LYP method employing a triple-ζ basis set (B3LYP/6-311G**//B1B95/6-31+G**) was used to compute molecular properties since this HDFT method was found by us to provide reliable optical transitions in nucleosides.[5-7] In Table S1 and S2 we have reported the electronic transitions having an oscillator strength *f* greater than 0.01.

References and Notes

(1) Hutton, A.; G. Roffi G.; Martelli, A. *Quad. Area Ric. Emilia Romagna,* **1974**, *5*, 67 – 74.

(2) Mulazzani, Q. G.; D'Angelantonio, M.; Venturi, M.; Hoffman, M. Z.; Rodgers, M. A. J. *J. Phys. Chem.* **1986**, *90*, 5347 – 5352.

(3) Buxton, G. V; Greenstock, C. L.; Helman, W. P.; Ross, A. B. *J. Phys. Chem. Ref. Data* **1988**, *17*, 513 – 886.

(4) Ross, A. B., Mallard, W. G.; Helman, W. P.; Buxton, G. V.; Huie, R. E.; Neta, P. *NDRLNIST Solution Kinetic Database - Ver. 3*, Notre Dame Radiation Laboratory, Notre Dame, IN and NIST Standard Reference Data, Gaithersburg, MD (1998).

(5) Chatgilialoglu, C.; Ferreri, C.; Bazzanini, R.; Guerra, M.; Choi, S.-Y.; Emanuel, C.J.; Horner, J.H.; Newcomb, M. *J. Am. Chem. Soc.* **2000**, *122*, 9525 – 9533.

(6) Chatgilialoglu, C.; Guerra, M.; Mulazzani, Q.G. *J. Am. Chem. Soc.* **2003**, *125*, 3839 – 3848.

(7) Chatgilialoglu, C.; Caminal, C.; Guerra, M.; Mulazzani, Q.G. *Angew. Chem. Int. Ed.* **2005**, *44*, 6030 – 6032.

(8) Becke, A. D. *Phys. Rev. A* **1988**, *38*, 3098 – 3100.

(9) Becke, A. D. *J. Chem. Phys.* **1996**, *104*, 1040 – 1046.

(10) Zhao, Y.; Pu, J.; Lynch, B. J.; Truhlar, D. G. *Phys. Chem. Chem. Phys.* **2004**, *6*, 673 – 676.

(11) Frisch, M. J.; Trucks, G. W.; Schlegel, H. B.; Scuseria, G. E.; Robb, M. A.; Cheeseman, J. R.; Montgomery, Jr., J. A.; Vreven, T.; Kudin, K. N.; Burant, J. C.; Millam, J. M.; Iyengar, S. S.; Tomasi, J.; Barone, V.; Mennucci, B.; Cossi, M.; Scalmani, G.; Rega, N.; Petersson, G. A.; Nakatsuji, H.; Hada, M.; Ehara, M.; Toyota, K.; Fukuda, R.; Hasegawa, J.; Ishida, M.; Nakajima, T.; Honda, Y.; Kitao, O.; Nakai, H.; Klene, M.; Li, X.; Knox, J. E.; Hratchian, H. P.; Cross, J. B.; Bakken, V.; Adamo, C.; Jaramillo, J.; Gomperts, R.; Stratmann, R. E.; Yazyev, O.; Austin, A. J.; Cammi, R.; Pomelli, C.; Ochterski, J. W.; Ayala, P. Y.; Morokuma, K.; Voth, G. A.; Salvador, P.; Dannenberg, J. J.; Zakrzewski, V. G.; Dapprich, S.; Daniels, A. D.; Strain, M. C.; Farkas, O.; Malick, D. K.; Rabuck, A. D.; Raghavachari, K.; Foresman, J. B.; Ortiz, J. V.; Cui, Q.; Baboul, A. G.; Clifford, S.; Cioslowski, J.; Stefanov, B. B.; Liu, G.; Liashenko, A.; Piskorz, P.; Komaromi, I.; Martin, R. L.; Fox, D. J.; Keith, T.; Al-Laham, M. A.; Peng, C. Y.; Nanayakkara, A.; Challacombe, M.; Gill, P. M. W.; Johnson, B.; Chen, W.; Wong, M. W.; Gonzalez, C.; and Pople, J. A. *Gaussian 03, Revision D.02*, Gaussian, Inc., Wallingford CT, 2004.

(12) Zhao, Y.; Lynch, B. J.; Truhlar, D. G. *J. Phys. Chem. A* **2004**, *108*, 2715 – 2719.

(13) Zhao, Y.; Truhlar, D. G. *J. Phys. Chem. A* **2004**, *108*, 6908 – 6918.

(14) Guerra, M. *Chem. Phys. Lett.* **1990**, *167*, 315 – 319.

(15) Guerra, M. *J. Phys. Chem. A* **1999**, *103*, 5983 – 5988.